

## Temperature and magnetic-field dependence of the $\text{Mn}^{2+} \ ^4T_1(^4G) \rightarrow \ ^6A_1(^6S)$ photoluminescence band in $\text{Zn}_{0.5}\text{Mn}_{0.5}\text{Se}$

J. F. MacKay, W. M. Becker, J. Spařek,\* and U. Debska<sup>†</sup>

*Department of Physics, Purdue University, West Lafayette, Indiana 47907*

(Received 29 December 1989)

The first and second moments of the  $\sim 2.15\text{-eV}$   $\text{Mn}^{2+}$  photoluminescence band in  $\text{Zn}_{0.5}\text{Mn}_{0.5}\text{Se}$  have been measured over the temperature range 4–300 K. The first moment of the  $\text{Mn}^{2+}$  emission band shows a red shift of  $\sim 12$  meV from 4 K to the minimum at  $\sim 45$  K, followed by a blue shift of  $\sim 40$  meV up to 300 K. The band position characterized by the first moment is found to be insensitive to an externally applied magnetic field of 6 T over the entire temperature range. These observations are interpreted in terms of the  $\ ^4T_1 \rightarrow \ ^6A_1$  optical transition accompanied by a pair of spin flips of neighboring  $\text{Mn}^{2+}$  ions. This model provides the correct magnitude of the temperature-dependent red shift for  $T \lesssim 50$  K, whereas lattice expansion accounts for the main part of the blue shift in the high-temperature regime,  $T \gtrsim 50$  K.

### I. INTRODUCTION

The ternary alloy  $\text{Zn}_{1-x}\text{Mn}_x\text{Se}$  is a member of the class of materials known as dilute magnetic semiconductors (DMS's).<sup>1</sup> In these materials the magnetic properties are primarily associated with a random substitution of  $\text{Mn}^{2+}$  for the  $\text{Zn}^{2+}$  cation. Even with no external magnetic field, the presence of the  $\text{Mn}^{2+}$  ions may manifest itself strongly in the optical properties of these crystals. For example, strong absorption bands due to  $\text{Mn}^{2+}$  intraion transitions are seen below the fundamental transition in the wide-gap DMS's. There has been much recent interest in the  $\text{Zn}_{1-x}\text{Mn}_x\text{Se}$  system, both for study of optical<sup>2</sup> and magnetic<sup>3</sup> effects observed in bulk crystals, as well as for optoelectronic-device possibilities in the blue region of the spectrum using heterostructures and superlattices grown by molecular-beam epitaxy (MBE).<sup>4</sup> In view of the technical interest, it is important to understand the basic optical properties of this system.

An extensively studied feature of DMS materials is the broad photoluminescence band due to the  $\text{Mn}^{2+} \ ^4T_1(^4G) \rightarrow \ ^6A_1(^6S)$  transition. Investigations of this band in  $\text{Cd}_{1-x}\text{Mn}_x\text{Te}$  (Refs. 5 and 6) and  $\text{Zn}_{1-x}\text{Mn}_x\text{Te}$  (Ref. 6) have shown an anomalous temperature dependence of the peak position of the  $\text{Mn}^{2+}$  emission band with temperature. For example, in  $\text{Cd}_{1-x}\text{Mn}_x\text{Te}$ , the peak position shifts to the red by  $\sim 40$  meV from 0 K to  $\sim 65$  K; the band then shifts back toward the blue by  $\sim 60$  meV upon further increasing the temperature to 300 K.

Müller and Gebhardt<sup>6</sup> and Heimbrodt *et al.*<sup>7</sup> have studied the photoluminescence in the antiferromagnetic phase of  $\text{Cd}_{1-x}\text{Mn}_x\text{Te}$  and  $\text{Cd}_{1-x}\text{Mn}_x\text{S}$ , respectively. They interpreted the temperature dependence of the line shift in terms of the mean exchange-field contribution to the energy of the ground and excited states. They show that the red shift in the low-temperature regime scales with the square of the sublattice magnetization in the antiferromagnetically ordered samples. However, they do

not address two principal questions: (i) the temperature at which the red shift disappears does not depend on the concentration of Mn ions while the Néel temperature does, and (ii) the shift is observed in systems which do not order antiferromagnetically.

The purpose of this paper is twofold: (1) to study the temperature and magnetic field dependences of the peak position of the  $\text{Mn}^{2+} \ ^4T_1 \rightarrow \ ^6A_1$  emission band in  $\text{Zn}_{1-x}\text{Mn}_x\text{Se}$  samples which do not order antiferromagnetically, and (2) to provide a theoretical interpretation of the line shift with temperature. In Sec. II we provide the details of our experiment, while Sec. III gives the experimental results. Section IV is a discussion and interpretation of our data with emphasis on two temperature regimes. The low-temperature regime,  $T \lesssim 45$  K, can be understood in terms of a shift induced by  $d$ - $d$  exchange interaction; the transition is interpreted as a  $d$ - $d$  transition within a single  $\text{Mn}^{2+}$  ion combined with a spin flip of one of the nearest neighbors. The model extends the theory used to explain magnon sidebands in antiferromagnetically ordered materials into the disordered region (at low and intermediate  $x$  values). Finally, it will be shown that the main part of the high-temperature behavior,  $T \gtrsim 45$  K, can be accounted for by the effect of lattice expansion on the  $\text{Mn}^{2+}$  energy-level scheme.

### II. EXPERIMENTAL DETAILS

The sample chosen for this investigation was grown by a modified Bridgman technique,<sup>8</sup> and was determined to be of the wurtzite structure by x-ray examination: microprobe analysis gave a manganese concentration of  $x = 0.5 \pm 0.01$ . Study of the  $\sim 2.15$  eV  $\text{Mn}^{2+}$  emission band in bulk  $\text{Zn}_{1-x}\text{Mn}_x\text{Se}$  is complicated by the presence of overlapping impurity bands at longer wavelengths. Two of the additional bands which appear in the alloy system are well known in  $\text{ZnSe}$  and  $\text{ZnSe:Mn}$ :<sup>9</sup> the Cu red emission ( $\sim 1.97$  eV) and the self-activated (SA) emission ( $\sim 2.05$  eV), either or both of which may be present in a

given sample. A third broad emission ( $\sim 1.7$  eV) of unknown origin is present in all samples. In the samples studied, these three bands are only present for  $T \gtrsim 45$  K and are thermally quenched for  $T \gtrsim 150$  K. In order to isolate the manganese emission band, the Cu was removed from the sample by the well-known Zn extraction technique.<sup>10</sup> The procedure is to anneal the crystal in pure molten Zn at 850°C for 1 week. While this method is effective in removing the Cu band, it has little effect on the SA band and no effect on the  $\sim 1.7$ -eV band. The presence of the SA emission could be detected by a deviation in the square of the half-width ( $H^2$ ) with temperature, since it causes increased broadening of the  $\text{Mn}^{2+}$  band. The data chosen for subsequent analysis were those showing minimal effect due to the presence of the long-wavelength bands. To confirm that the first moment of the  $\text{Mn}^{2+}$  band is unaffected by the annealing process, the same measurements were done on samples grown by MBE that were uncontaminated by either Cu or SA emission bands. The results for the MBE samples<sup>11</sup> are consistent with those to be discussed here.

Spectra were taken using a Spex 1407 1/4-m monochromator and a cooled RCA 31034 photomultiplier tube with a GaAs photocathode. Excitation was into the  ${}^6A_1({}^6S) \rightarrow {}^4T_2({}^4G)$  absorption region using the 488-nm line of an argon laser. A 6-T external magnetic field was applied in a Janis superconducting magnet. Spectra were taken in 0.5-nm steps and corrected for the response of the detection system to give the true line shape of the emission band. The integrated intensity or zeroth moment of the emission band is defined as

$$M^{(0)} = \int I(E) dE, \quad (1)$$

where  $I(E)$  is the intensity at the energy  $E$ . The first moment or average energy of the band is

$$M^{(1)} = \frac{\int EI(E) dE}{M^{(0)}}. \quad (2)$$

The second moment is calculated using the above relations:

$$M^{(2)} = \frac{\int (E - M^{(1)})^2 I(E) dE}{M^{(0)}}. \quad (3)$$

Finally, the square of the full width at half maximum is calculated from the second moment by using the relation

$$H^2 = (8 \ln 2) M^{(2)}. \quad (4)$$

Care was taken to subtract out the baseline noise before calculating the first moment, since the data were integrated over a finite energy range. The errors in the calculation of the first moment were largest between 100 and 150 K, where the  $\sim 1.7$ -eV band made a small contribution to the long-wavelength component of the apparent  $\text{Mn}^{2+}$  emission. This contribution has the effect of shifting the apparent peak position of the  $\text{Mn}^{2+}$  band to lower energy. Data taken in a single run varied smoothly with temperature; however, successive runs showed that the curves shifted up or down by a few meV, perhaps due to inhomogeneities in the sample. In the magnetic field

studies, successive measurements were made for 0 and 6 T at fixed temperature to minimize beam wandering and thermal instabilities.

### III. EXPERIMENTAL RESULTS

Below we present the results of our study of the temperature and magnetic field dependence of the first and second moments of the  $\text{Mn}^{2+}$  emission band in  $\text{Zn}_{0.5}\text{Mn}_{0.5}\text{Se}$  (subsection A). The measurements are validated in subsection B, where we show that anomalous broadening of the emission band does not account for the shift of the first moment with temperature.

#### A. Photoluminescence

The photoluminescence spectra of the  $\text{Mn}^{2+} {}^4T_1 \rightarrow {}^6A_1$  emission band are shown in Fig. 1 at three temperatures: 4.2, 48, and 150 K. These spectra illustrate the observed shift in the band and indicate that the band shape is nearly Gaussian with a long-wavelength tail. The inset in Fig. 1 shows the presence of both the  $\sim 1.7$ -eV band and the  $\text{Mn}^{2+}$  emission band at 120 K: at this temperature some overlap between the two bands is observed.

Figure 2(a) shows the first moment of the  $\text{Mn}^{2+}$  emission band as a function of temperature. For  $T \lesssim 15$  K the first moment is insensitive to temperature. A shift to the red occurs with increasing temperature and is clearly observable for  $T > 20$  K, with an average decrease of  $\sim 12$  meV between 4 K and the minimum at  $\sim 45$  K. This shift is less than half the  $\sim 40$  meV observed in  $\text{Cd}_{1-x}\text{Mn}_x\text{Te}$ ,<sup>5,6</sup> and the temperature at which the minimum of energy occurs is lower than the 60 K reported in  $\text{Cd}_{1-x}\text{Mn}_x\text{Te}$ . Above  $\sim 45$  K the peak position

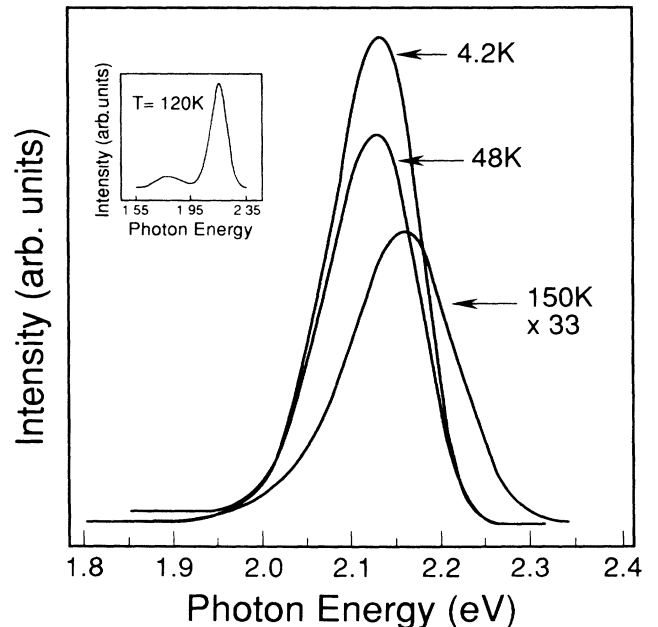


FIG. 1.  $\text{Zn}_{0.5}\text{Mn}_{0.5}\text{Se}$ :  $\text{Mn}^{2+} {}^4T_1 \rightarrow {}^6A_1$  emission band at  $T = 4.2, 48,$  and  $150$  K. Inset shows the  $\text{Mn}^{2+}$  emission band along with the unknown  $\sim 1.7$ -eV emission band.

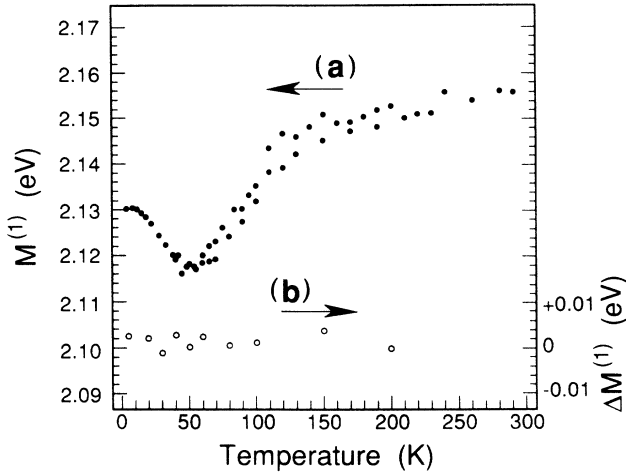


FIG. 2.  $\text{Zn}_{0.5}\text{Mn}_{0.5}\text{Se}$ : (a)  $M^{(1)}$  vs temperature; (b)  $\Delta M^{(1)}$  vs temperature.  $M^{(1)}$  is the first moment or average energy of the band.  $\Delta M^{(1)}$  is the change in the first moment,  $M^{(1)}(6 \text{ T}) - M^{(1)}(0)$ .

moves toward the blue with a total change of  $\sim 40$  meV between the minimum and room temperature. The blue shift here is again less than that observed in  $\text{Cd}_{1-x}\text{Mn}_x\text{Te}$ , as noted earlier. Figure 2(b) gives the change in the first moment,

$$\Delta M^{(1)} = M^{(1)}(6 \text{ T}) - M^{(1)}(0), \quad (5)$$

in an external magnetic field of 6 T and in the temperature range 4.2–300 K. No systematic effect due to the external field is discernible within our resolution of  $\pm 1$  meV. A similar conclusion has been reached by Lee *et al.*<sup>12</sup> who studied the optical-absorption spectra of  $\text{Zn}_{0.55}\text{Mn}_{0.45}\text{Se}$  in fields up to 15.58 T.

Figure 3(a) shows the change in the full width at half maximum squared ( $H^2$ ) of the  $\text{Mn}^{2+}$  band with temperature. Figure 3(b) is a plot of  $\Delta H^2$  as a function of temperature, where

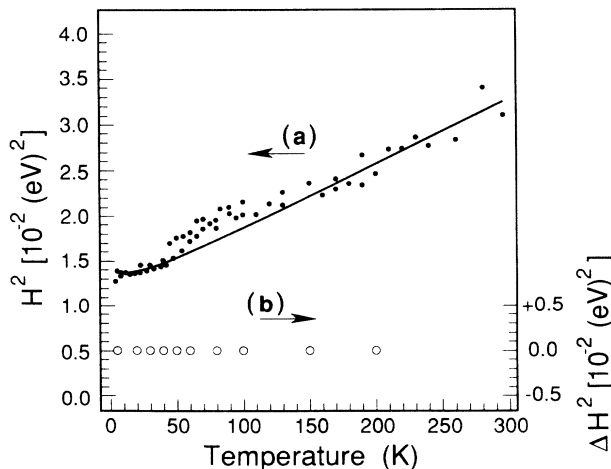


FIG. 3.  $\text{Zn}_{0.5}\text{Mn}_{0.5}\text{Se}$ : (a)  $H^2$  vs temperature; (b)  $\Delta H^2$  vs temperature.

$$\Delta H^2 = H^2(6 \text{ T}) - H^2(0). \quad (6)$$

As with the first moment,  $H^2$  is insensitive to the external magnetic field.

### B. Line broadening

Any attempt to measure the first moment must take into account line shape, particularly when other bands may be present. Rather than attempt deconvolution of the bands, we assume thermal broadening due to vibronic interaction and examine the data for unexpected deviations. For a strong linear interaction, theory predicts a Gaussian line shape with a full width at half maximum  $H(T)$  given by the semiclassical expression<sup>13</sup>

$$H^2(T) = H^2(0) \coth \left[ \frac{\hbar\omega}{2kT} \right] + H_{\text{in}}^2. \quad (7)$$

Here we have set the ground- and excited-state vibrational frequencies  $\omega_g = \omega_e = \omega$ . The term  $H_{\text{in}}$  is the inhomogeneous broadening arising due to transitions involving a distribution of emitting states. In Fig. 3 we give a fit to the measured half-width data using the above relation. Good agreement is obtained using the following parameters:  $\hbar\omega = 6.0 \pm 1$  meV,  $H_{\text{in}} = 0.11$  eV,  $H^2(0) = (8 \ln 2)S(\hbar\omega)^2 = 2.5 \times 10^{-3}$  eV<sup>2</sup>, and  $S = 12.5$ . Note the upward concavity for  $50 \leq T \leq 100$  K in the otherwise convex plot of  $H^2$  versus temperature; this is ascribed to residual SA contamination. As a result, the above fit was performed avoiding half-width data between 50 and 100 K. The effect of the SA-induced broadening is to decrease the energy of the first moment for  $50 \leq T \leq 100$  K, so that the blue shift for  $T > 50$  K should occur more rapidly than our data would indicate. In other samples investigated, the broadening due to the SA emission was much larger; in some cases  $H^2$  would increase by a factor of 2, resulting in a pronounced maximum in  $H^2$  for  $T \approx 80$  K and a shift in the minimum of  $M^{(1)}$  to  $T \approx 80$  K. We may conclude from Fig. 2(a) that the variation of  $H^2$  with temperature gives no indication that anomalous broadening produces the shifts observed in the peak position.

## IV. DISCUSSION AND INTERPRETATION

Attempts to explain the shift of the peak position of the  $\text{Mn}^{2+}$  emission band with temperature in  $\text{Cd}_{1-x}\text{Mn}_x\text{Te}$  (Refs. 5 and 6) and  $\text{Zn}_{1-x}\text{Mn}_x\text{Te}$  (Ref. 6) have met with limited success. Moriwaki *et al.*<sup>5</sup> were unable to explain the band shift for  $T \lesssim 60$  K, but they suggested that the blue shift for  $T \gtrsim 60$  K might originate in temperature-dependent energy transfer between emitting  $\text{Mn}^{2+}$  ions. Müller and Gebhardt<sup>6</sup> argued that the red shift for  $T \lesssim 60$  K was related to the antiferromagnetic ordering by showing that the low-temperature band shift scales with the square of the sublattice magnetization up to the Néel temperature of 45 K. However, the red shift has also been observed in samples which do not order antiferromagnetically, so a more general explanation must be provided. These authors also concluded it was unlikely that the superexchange interaction between  $\text{Mn}^{2+}$  ions

caused the observed low-temperature band shift, but suggested that the  $s$ - $d$  and  $p$ - $d$  exchange interaction might be used to explain the shift if there were strong hybridization of the Mn  $3d$  and Te  $5p$  wave functions. Below we provide a model which explains the low-temperature shift, taking into account  $d$ - $d$  interactions only. Later, we show that the high-temperature shift is primarily due to the influence of lattice expansion on the crystal-field levels. Finally, we compare the proposed model involving  $d$ - $d$  exchange interactions with that of the bound-magnetic-polaron state.

#### A. Shift of $M^{(1)}$ with temperature for $T \lesssim 50$ K

The question is how to interpret the temperature dependence of the  $d$ - $d$  transition in  $\text{Zn}_{1-x}\text{Mn}_x\text{Se}$  and related materials. One should realize that the wave functions in the ground ( ${}^6A_1$ ) and excited ( ${}^4T_1$ ) states are substantially different in these two systems; the former is spherically symmetric, obeying Hund's rule, ( $L=0, S=\frac{5}{2}$ ), whereas the latter corresponds to an ( $S=\frac{3}{2}, L\neq 0$ ) excited state. The excited-state configuration ( ${}^4T_1$ ) corresponds to the spin flip of one of the five  $3d$   $\text{Mn}^{2+}$  electrons which are coupled by the Hund's-rule exchange. We interpret the luminescence spectra as the  ${}^4T_1 \rightarrow {}^6A_1$  deexcitation combined with a spin flip of one of the nearest-neighbor  $\text{Mn}^{2+}$  ions and propose the following picture. In the excited state, the central  $\text{Mn}^{2+}$  ion with one electron in the  ${}^4T_1$  state is surrounded, on average, by  $zx$  magnetic nearest neighbors, where  $z$  is the total number of available nearest-neighbor cation sites for each  $\text{Mn}^{2+}$  ion. In this state, which is one of the crystal-field states, the value of the spin is approximately  $\frac{3}{2}$ . The electron undergoes a transition back to the ground state with a simultaneous spin flip of one of the neighboring  $\text{Mn}^{2+}$  ions via pair antiferromagnetic superexchange interaction. The remaining neighbors provide an additional magnetic polarization that also influences the energy of the transition; this additional polarization can be calculated in the mean-field approximation. Thus the total change in energy of the transition due to exchange interaction is

$$\Delta E_{\text{ex}} = \Delta E_{\text{pair}} + \Delta E_{\text{MF}}, \quad (8)$$

where  $\Delta E_{\text{pair}}$  and  $\Delta E_{\text{MF}}$  are, respectively, the pair-spin-flip and the mean-field contributions to the total exchange energy. This mechanism is schematically drawn in Fig. 4, where the transition corresponds to the total change of the  $z$ -spin component  $\Delta S_T^z = 0$  since the flips are in opposite directions. The condition  $\Delta S_T^z = 0$  is required for the electric dipole transition to be allowed.<sup>14</sup> Note that the  $\text{Mn}^{2+}$  ion in  $\text{Zn}_{1-x}\text{Mn}_x\text{Se}$  has no inversion symmetry; therefore the transition is parity allowed. The pair of spin flips is induced by the transverse part,  $\sim (S_1^+ S_2^- + S_1^- S_2^+)$ , of the exchange interaction between the two involved magnetic ions. In addition, the pair of spin flips evolves into a two-magnon sideband in the absorption spectrum when the system orders antiferromagnetically (e.g., for  $x \gtrsim 0.6$  in  $\text{Cd}_{1-x}\text{Mn}_x\text{Te}$ ).<sup>14</sup>

To estimate the exchange-interaction contribution to

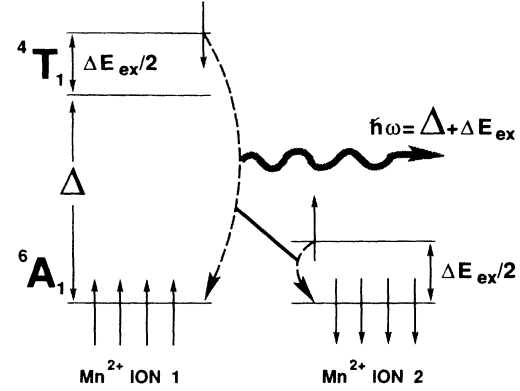


FIG. 4. Schematic representation of the  $d$ - $d$  photoluminescence transition in  $\text{Mn}^{2+}$  ion 1 combined with the spin flip of a neighboring  $\text{Mn}^{2+}$  ion 2 coupled to ion 1 by antiferromagnetic exchange interaction.  $\Delta$  is the energy of the crystal-field splitting and  $\Delta E_{\text{ex}}$  is the total change due to the exchange interaction, while  $\Delta E_{\text{ex}}/2$  is the corresponding change per spin. The transition is of electric dipole type.

the transition depicted in Fig. 4, we note that the exchange energy for the  $\text{Mn}^{2+}$  pair is

$$2JS_1 \cdot S_2 = J[(S_1 + S_2)^2 - S_1^2 - S_2^2] \\ = J[S_T(S_T + 1) - S_1(S_1 + 1) - S_2(S_2 + 1)]. \quad (9)$$

The total spin for the pair in the ground state is  $S_T = 0$ , whereas, in the excited state,  $S_T = 1$ . In the excited state,  $S_1 = \frac{3}{2}$  and  $S_2 = \frac{5}{2}$ , while, in the ground state,  $S_1 = S_2 = \frac{5}{2}$ . Therefore, the energy difference in these two configurations is  $\Delta E_{\text{pair}} = 7|J|$ . The exchange integral for  $\text{Zn}_{1-x}\text{Mn}_x\text{Se}$  is  $J \simeq -13.5$  K (Ref. 3), giving  $\Delta E_{\text{pair}} \simeq 95$  K  $\simeq 8$  meV. For  $\text{Cd}_{1-x}\text{Mn}_x\text{Te}$ ,  $J \simeq -7.5$  K, so that  $\Delta E_{\text{pair}} \simeq 50$  K. Note that these numbers are only approximate estimates—the value of the exchange integral in the excited state may differ from the corresponding value for the ground state. Hence, in general,

$$\Delta E_{\text{pair}} = \frac{1}{2}|35J - 21J'|. \quad (10)$$

Here,  $J'$  and  $J$  are the superexchange integrals in the excited and ground states, respectively. In the above estimate we take  $J' = J$ .

The exchange contribution to the transition due to the pair-exchange coupling will be important only up to the temperature at which  $k_B T = k_B T_{\text{min}} \simeq \Delta E_{\text{pair}}$ . Above this characteristic temperature, the exchange coupling is destroyed by the thermodynamic fluctuations of the spins; that is, the electron in the excited state is surrounded by approximately an equal number of up and down spins.

The important feature of the considered transitions is that  $\Delta E_{\text{pair}}$  does not represent the total exchange contribution to the transition energy. This is because the excited  $\text{Mn}^{2+}$  ions are surrounded, in general, by more than one nearest-neighbor  $\text{Mn}^{2+}$  ion, particularly for  $x > 0.1$ . To calculate the total exchange contribution, we treat all the remaining  $(z-1)x$  magnetic neighbors in the mean-field approximation, which may be expressed as

$$\Delta E_{\text{MF}} = \sum'_{i \neq j} J_{ij} \langle \mathbf{S}_i \cdot \mathbf{S}_j \rangle \approx 2J(z-1)x \langle \mathbf{S}_i \rangle \cdot \langle \mathbf{S}_j \rangle, \quad (11)$$

where the primed summation means that we take into account only  $(z-1)x$  magnetic neighbors. Next, we calculate the change of this energy under a spin flip of a single electron. If the spin is flipped in the ground-state configuration, then the energy change is

$$J(z-1)xS(\frac{1}{2}) - J(z-1)xS(-\frac{1}{2}) = J(z-1)xS. \quad (12)$$

Analogously, the corresponding change in energy if  $J \neq J'$  is

$$J'(z-1)xS(\frac{1}{2}) - J(z-1)xS(-\frac{1}{2}) = \frac{1}{2}|J' + J|(z-1)xS. \quad (13)$$

Combining Eqs. (12) and (13) with Eq. (10) and taking  $J' = J$ , we find that the total energy change is

$$\Delta E_{\text{ex}} = \Delta E_{\text{pair}} + 2|J|x(z-1)S. \quad (14)$$

For  $\text{Zn}_{0.5}\text{Mn}_{0.5}\text{Se}$ ,  $\Delta E_{\text{ex}} = 320 \text{ K} \sim 28 \text{ meV}$ , a reasonable number in view of the crudeness of our estimate. Note that  $T_{\text{min}}$  does not depend on  $x$ , whereas the total low-temperature shift does;  $\Delta E_{\text{ex}} = a + bx$ . Both features are in agreement with our observations.<sup>11</sup>

The very nature of the proposed transitions excludes the magnetic field dependence in the same way as two-magnon Raman scattering in two-sublattice antiferromagnets.<sup>15</sup> Explicitly, the energy of the pair of spins in the excited state in a magnetic field can be written as

$$E = J[S_T(S_T + 1) - \frac{25}{2}] + g^* \mu_B \mathbf{B} \cdot \mathbf{S}_1 + g \mu_B \mathbf{B} \cdot \mathbf{S}_2, \quad (15)$$

where  $g \approx 2$  and  $g^*$  is the Landé factor in the excited state. Since  $g^* \approx g$ , we have

$$E = J[S_T(S_T + 1) - \frac{25}{2}] + g \mu_B B(S_1^z + S_2^z). \quad (16)$$

The magnetic field independence of the transition energy is implied by the circumstance that the concomitant change of the z-spin component is zero, i.e.,  $\Delta S_1^z + \Delta S_2^z = 0$ .

### B. Shift of $M^{(1)}$ with temperature: $50 \lesssim T \lesssim 300 \text{ K}$

We consider the possibility that thermal-expansion effects influence the ligand field and thus may give rise to the observed shifts of  $M^{(1)}$  with temperature for  $T \geq 50 \text{ K}$ . This is consistent with pressure studies on DMS's, which yield negative pressure coefficients for the linear term in  $E(P)$  for the  $\text{Mn}^{2+} \ ^6A_1 \rightarrow \ ^4T_1$  (Refs. 16–19),  $\ ^6A_1 \rightarrow \ ^4T_2$  (Refs. 16 and 20), and  $\ ^6A_1 \rightarrow \ ^4A_1, \ ^4E$  (Refs. 16, 20, and 21) absorption, and  $\ ^4T_1 \rightarrow \ ^6A_1$  emission features (Refs. 16 and 17). From these results values of the pressure dependence of relevant quantities may be derived: the crystal-field parameter  $Dq$  and the Racah parameters  $B$  and  $C$ . Because of incomplete information on the pressure derivatives, we turn directly to experiment. Several investigations<sup>16,17</sup> show that  $dE/dP \sim -(40-80) \text{ meV/GPa}$  for the  $\ ^4T_1 \rightarrow \ ^6A_1$  transition in various DMS's. Linear- or volume-expansion coefficients for the

$\text{Zn}_{1-x}\text{Mn}_x\text{Se}$  alloy system are not available in the literature. However, data given by Zhdanova and Sergeev show<sup>22</sup> that in ZnSe the linear-expansion coefficient  $\alpha$  undergoes a monotonic increase in value from 80 to 600 K, with  $\alpha(77 \text{ K}) \approx 2.5 \times 10^{-6} \text{ deg}^{-1}$  and  $\alpha(600 \text{ K}) \approx (7-8) \times 10^{-6} \text{ deg}^{-1}$ . Integrating between 77 and 300 K gives a fractional change in lattice constant of  $\sim +1.6 \times 10^{-3}$ ; other results<sup>23</sup> suggest that for MnSe in the NaCl structure the fractional change is doubled. Based on these results, we assume that, for  $x=0.5$ ,  $\Delta a/a \approx 2.5 \times 10^{-3}$  in the same temperature range. Using a value of compressibility of  $\kappa = 0.01946 \text{ GPa}^{-1}$ , we estimate the effective pressure change (in GPa) to be

$$dP = -\frac{dV}{V} \frac{1}{\kappa} = +0.385. \quad (17)$$

The compressibility results were calculated<sup>24</sup> from elastic-constant measurements given in Ref. 25. Such a change would then produce a line shift of  $\sim +23 \text{ meV}$ , in rough agreement with our observations, which give  $\sim 40 \text{ meV}$ . It is tempting to apply this model to the region  $T < 50 \text{ K}$ , since negative values of the linear-expansion coefficient are seen in ZnSe and other semiconductors at low temperatures.<sup>26</sup> This can be ruled out, since the  $\alpha$  values are too small and should give an integrated effect 2 orders of magnitude less than observed.

### C. Comparison to the bound magnetic polaron

The intriguing feature of the temperature dependence of  $M^{(1)}$  presented in Fig. 2 is the similarity to the temperature dependence of the spin splitting for the bound-magnetic-polaron (BMP) state.<sup>27</sup> This analogy is supported by the circumstance that  $2p \rightarrow 3d$  transitions may occur in the same energy range.<sup>12</sup> In this case the emission would take place between the  $3d^6$  state and  $2p^5$  hole polaron state. In Fig. 5 we have plotted the first moment as a function of  $\chi(T)T$ , where  $\chi(T)$  is the magnetic susceptibility. If magnetic polaron effects or other magnetic

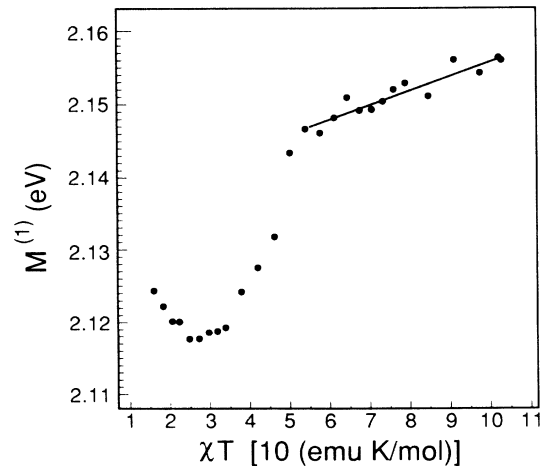


FIG. 5. First moment of the emission line as a function of  $\chi(T)T$ , where  $\chi(T)$  is the magnetic susceptibility of the  $\text{Zn}_{0.5}\text{Mn}_{0.5}\text{Se}$  sample.

moment fluctuations were of importance, then the high-temperature part of the data should show a linear dependence on temperature:  $M^{(1)} = A[\chi(T)T] + B$ . A fit to our data yields  $A = 1.94 \times 10^{-3}$  eV mol/emu K and  $B = 2.136$  eV. However, this interpretation of the transition as the  $2p \rightarrow 3d$  transition with a BMP state in the excited state can easily be ruled out since the BMP energy would depend strongly on the magnitude of the applied magnetic field.

In the model we have proposed, the magnetic part of the transition energy is rather that of an *atomic* magnetic polaron undergoing a spin-flip exchange with one of its neighboring spins. We call this object composed of the excited  $Mn^{2+}$  ion surrounded by the same ions in the ground state the atomic version of the bound-magnetic-polaron state, since both the central and surrounding spins are localized atomic spins. Under these conditions, the magnetic part of the energy in the high-temperature regime (well above  $T_{min}$ ) can be expressed in the same way as the BMP,

$$\Delta E = A\chi(T)T + B(T), \quad (18)$$

where the first term is connected with the thermodynamic fluctuations of the surrounding spins and the second term contains the crystal-field splitting.

One should also mention that the present interpretation may be used to explain Raman scattering involving pairs of antiferromagnetically coupled  $Mn^{2+}$  ions in DMS's.<sup>28</sup> The simplest Stokes-scattering process involves the creation of a pair of spin flips in the final state with  $\Delta S_T = 1$  and  $\Delta S_T' = 0$ . Then, according to Eq. (16), the Stokes-line position will not depend on the external magnetic field.

## V. SUMMARY

The retrograde thermal shift of the first moment of the  $\sim 2.15$ -eV  $Mn^{2+} \ ^4T_1 \rightarrow \ ^6A_1$  band has been determined in a bulk crystal of  $Zn_{0.5}Mn_{0.5}Se$ . Ambiguities in the results due to overlapping extrinsic emissions have been removed by careful sample selection and processing, by the analysis of residual effects due to these emissions, and by comparison with behavior observed in samples made by the MBE technique.<sup>11</sup> No magnetic field dependence for either the first or second moments of the  $\ ^4T_1 \rightarrow \ ^6A_1$  band was detected.

A new model appropriate for the antiferromagnetically disordered region of the alloy concentration has been proposed to explain (1) the  $x$  independence of the temperature at which the red shift disappears, and (2) the magnetic field independence of the first moment. The model invokes an electronic transition of an excited  $Mn^{2+}$  ion to the ground state with the simultaneous spin flip of one of the neighboring  $Mn^{2+}$  ions, with an energy shift occurring via pair-exchange interaction. Lattice-dilatational effects estimated from high-pressure data, elastic-constant results, and thermal expansion have been used to explain the blue shift of the first moment at high temperatures.

## ACKNOWLEDGMENTS

The authors wish to thank A. Lewicki for providing the magnetic-susceptibility data. We are also grateful to R. Alonzo and E. Oh for their assistance with the magnetic field measurements. Useful comments of R. R. Gałazka are appreciated. This work was supported by the U.S. National Science Foundation under Grant No. DMR-85-20866.

\*On leave from Department of Solid State Physics, Akademia Górniczo-Hutnicza (AGH) Technical University, PL-30-059 Krakow, Poland.

†Permanent address: Institute of Theoretical Physics, Warsaw University, ulica Hoża 69, PL-00-681 Warszawa, Poland.

<sup>1</sup>For recent reviews, see J. K. Furdyna, *J. Appl. Phys.* **64**, R29 (1988); N. B. Brandt and V. V. Moshchakalkov, *Adv. Phys.* **33**, 193 (1984).

<sup>2</sup>R. B. Bylsma, W. M. Becker, J. Kossut, and U. Debska, *Phys. Rev. B* **33**, 207 (1986).

<sup>3</sup>J. K. Furdyna, N. Samarth, R. B. Frankel, and J. Spałek, *Phys. Rev. B* **37**, 3707 (1988); A. Twardowski, M. von Ortenberg, M. Demianiuk, and R. Pauthenet, *Solid State Commun.* **51**, 849 (1984).

<sup>4</sup>L. A. Kolodziejski, R. L. Gunshor, N. Otsuka, S. Datta, W. M. Becker, and A. V. Nurmikko, *IEEE J. Quantum Electron.* **QE-22**, 1666 (1986).

<sup>5</sup>M. M. Moriwaki, W. M. Becker, W. Gebhardt, and R. R. Gałazka, *Phys. Rev. B* **26**, 3165 (1982).

<sup>6</sup>E. Müller and W. Gebhardt, *Phys. Status Solidi B* **137**, 259 (1986).

<sup>7</sup>W. Heimbrodt, C. Benecke, O. Goede, and H. E. Gumlich, *Phys. Status Solidi B* **154**, 405 (1989).

<sup>8</sup>U. Debska, W. Giriat, H. R. Harrison, and D. R. Yoder-Short,

*J. Cryst. Growth* **70**, 399 (1984).

<sup>9</sup>G. Jones and J. Woods, *J. Phys. D* **6**, 1640 (1973); G. Jones and J. Woods, *J. Lumin.* **9**, 389 (1974).

<sup>10</sup>M. Aven and H. H. Woodbury, *Appl. Phys. Lett.* **1**, 52 (1962).

<sup>11</sup>J. F. MacKay, W. M. Becker, J. Spałek, L. A. Kolodziejski, and R. L. Gunshor (unpublished).

<sup>12</sup>Y. R. Lee, A. K. Ramdas, and R. L. Aggarwal, *Phys. Rev. B* **38**, 10 600 (1988).

<sup>13</sup>T. H. Keil, *Phys. Rev.* **140**, A601 (1965).

<sup>14</sup>Compare, e.g., D. D. Sell, *J. Appl. Phys.* **39**, 1030 (1965); T. Moriya, *ibid.* **39**, 1042 (1965).

<sup>15</sup>P. A. Fleury and R. Loudon, *Phys. Rev.* **156**, 514 (1968).

<sup>16</sup>K. Hochberger, H. H. Otto, and W. Gebhardt, *Solid State Commun.* **62**, 11 (1987).

<sup>17</sup>E. Müller, W. Gebhardt, and W. Rehwald, *J. Phys. C* **16**, L1141 (1983).

<sup>18</sup>W. Shan, S. C. Shen, and H. R. Zhu, *Solid State Commun.* **55**, 475 (1985).

<sup>19</sup>G. Ambrazevičius, G. Babonas, S. Marcinkevičius, V. D. Prochukhan, and Y. V. Rud, *Solid State Commun.* **49**, 651 (1984).

<sup>20</sup>J. Shan, S. C. Shen, L. Qiquang, Z. Haorong, and J. Quanglin, *Solid State Commun.* **70**, 1 (1989).

<sup>21</sup>S. Ves, K. Strössner, W. Gebhardt, and M. Cardona, *Solid State Commun.* **57**, 335 (1986).

- <sup>22</sup>V. V. Zhadanova and V. P. Sergeev, *Fiz. Tverd. Tela* (Leningrad) **14**, 2153 (1972) [*Sov. Phys.—Solid State* **14**, 1859 (1973)].
- <sup>23</sup>W. F. Pong, R. A. Mayanovic, B. A. Bunker, J. K. Furdyna, and U. Debska, *Phys. Rev. B* **41**, 8440 (1990).
- <sup>24</sup>R. J. Sladek (private communication).
- <sup>25</sup>R. A. Mayanovic, R. J. Sladek, and U. Debska, *Phys. Rev. B* **32**, 1311 (1988).
- <sup>26</sup>T. F. Smith and G. K. White, *J. Phys. C* **8**, 2031 (1975).
- <sup>27</sup>J. Spałek and J. Kossut, *Solid State Commun.* **61**, 483 (1987); T. Dietl and J. Spałek, *Phys. Rev. Lett.* **48**, 355 (1982).
- <sup>28</sup>D. U. Bartholomew, E.-K. Suh, S. Rodriguez, and A. K. Ramdas, *Solid State Commun.* **62**, 235 (1987).

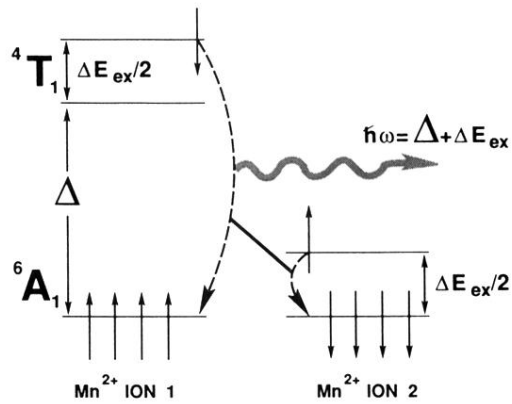


FIG. 4. Schematic representation of the  $d-d$  photoluminescence transition in  $Mn^{2+}$  ion 1 combined with the spin flip of a neighboring  $Mn^{2+}$  ion 2 coupled to ion 1 by antiferromagnetic exchange interaction.  $\Delta$  is the energy of the crystal-field splitting and  $\Delta E_{ex}$  is the total change due to the exchange interaction, while  $\Delta E_{ex}/2$  is the corresponding change per spin. The transition is of electric dipole type.